HTWK Leipzig University of Applied Sciences

ING Faculty of Engineering

# An Efficient Low-Power Wake-Up Receiver Architecture for Power Saving for Transmitter and Receiver Communications

Robert Fromm, Lydia Schott and Faouzi Derbel

Note: This is the manuscript version of this publication. See https://doi.org/10.5220/0010236400610068 for the published version. Current version: October 26, 2022.

**Abstract**

For power-limited wireless sensor networks, energy efficiency is a critical concern. Receiving packages is proven to be one of the most power-consuming tasks in a WSN. To address this problem the asynchronous communication is based on wake-up receivers. The proposed receiver circuit can detect carrier signals inside the 868 MHz band. Reliable signal detection at 10 m was achieved with a total power consumption of 4.2 µW. Two use cases of this low-power receiver were introduced. First the wake-up receiver and second as a collision avoidance circuit. Because of its low power consumption savings of factor 7000 can be estimated compared to integrated solutions of commercially available radio transceivers.

**Keywords**

wake-up receiver (WuRx), wireless sensor network (WSN), ultra-low power (ULP), collision avoidance, carrier sensing, energy detection, passive RF architecture, operational amplifier (Op-Amp), comparator, Schottky diode, envelope detector.

## 1 Introduction

The design of wireless sensor networks based on sensor nodes with low power consumption requires the development of highly energy-efficient systems, especially for continuous operations. The communication between sensor nodes can be classified into three categories: synchronous, pseudo-synchronous, and asynchronous [Ban16]. In synchronous networks, the nodes synchronize their clocks to wake up from sleep mode simultaneously. In a pseudo-asynchronous scheme,

the sender transmits a preamble before sending the data, which checks that the receiver is ready to receive data [Ple08].
The asynchronous communication is used with a duty cycle operation, where three modes are generally introduced: short receiving mode, application-oriented transmission mode, and a long sleeping mode. This kind of communication is usually used for energy autarkic sensor nodes allowing a long operating time. The drawback related to this kind of communication is latency and reaction time related to the sleeping modes, where the node is not able to communicate due to the high current consumption of recent high-frequency transceivers. These receivers require a high amount of energy, taking more than 70 % out of the battery [BDK18b]. By introducing energy-efficient receivers with a current consumption in the range of a few microamperes allowing a continuous receiving. This kind of receivers are known as wake-up receivers. It is generally added to the main sensor node. During the idle mode, only the wake-up receiver is active and is waiting for telegrams with its appropriate identifier. Once a telegram with the intended identifier is received, an interrupt will be generated and the main node is changing from sleeping to active mode.
The architecture of a wake-up receiver is generally based on passive components and amplifiers with low power consumption. Those components are followed by an active component, allowing the matching to the unique identifier, to generate the interrupt for the main transceiver. The main component of a wake-up receiver is the envelope detector for the demodulation of received signals. Schottky diodes are a good choice for this purpose due to their capability to demodulate on-off keying (OOK) signals passively [BDK18a] [Spe+15]. Limitation in terms of sensitivity will be improved by using appropriate amplifiers. Due to its continuous operating, passive wake-up receivers detect the activity in the communication channel and cannot distinguish a wake-up signal from other RF activity [Mag+16]. The main drawback of recent passive architecture is therefore the late decision whether the telegram belongs to the wake-up receiver or not. With the help of a carrier sense circuit, the occupancy of the channel can be observed continuously. This way the interferences between multiple wake-up-capable systems could be minimized. With this approach, unnecessary power consumption due to lost packages through interference can be reduced. This is intensified especially in active and dense networks operating in the same frequency band.
In this paper, a power-saving architecture for a wake-up receiver and the corresponding transmitter is presented. The logic is completely located in the operational amplifiers and comparator, which sends the interrupt to the microcontroller without addressing it.

The paper is structured as follows: Section 2 gives an overview of related works. The concept of the used components is presented in section 3. Section 4 presents the circuit design and measurements in diode comparison and current consumption. The conclusion and a further outlook are found in section 5.

## 2 Related Works

For more than a decade a lot of research has been done in the field of wake-up radios. [DP+16] introduces a dual-band wake-up radio that enables interoperability with the two most commonly used bands in the wireless sensors networks and Internet of Things (IoT). The simulation results show a system with a sensitivity of up to –55 dBm at 868 MHz and –53 dBm at 2.4 GHz. A comparator with very low power consumption and a small input offset voltage is used to reproduce the rectified wake-up message.
Three different comparators to evaluate the trade-off between performance and sensitivity were analyzed by [Mag+16]. The signal generated by the envelope detector is converted into a digital envelope by a semi-passive interrupt generator with a comparator as an active component. The wake-up receiver reaches a sensitivity of up to –55 dBm at a maximum power of 1.2 µW. To avoid a wrong wake-up a logic circuit, which filters the data can be used. [Pol+16] uses an 8-bit PIC microcontroller to generate the final wake-up signal to the main controller. The idle power consumption is 400 nW and increase up to 63 µW when receiving data.
In [ABD15] an address decoder block with low power consumption and minimal latency is introduced. The decoder is based on logical flip-flops. As soon as the data in the flip-flops matches with the preset identifier in a memory register, an interrupt is sent to the main transceiver. In active mode, the code detector consumes 13.41 µW at 0.9 V, while in sleep mode it has no power consumption. An ultra-low-power digital basebad (DBB), based on a low power microcontroller, is presented in [BBD18]. Instead of constantly monitoring the channel, the PC12LF1572 microcontroller periodically wakes up and activates the remaining WuRx components. For a latency of $T_S = 32$ ms, the DBB consumes less than 1 µW. [BD14] introduces a nanowatt wake-up receiver (WuRx) and compares the power consumption of two techniques of address decoding. The presented WuRx consumes nearly 230 nA and communication range can reach up to 15 m at a transceiving power of 25 dBm.
This paper describes a wake-up receiver architecture based on passive components allowing an improvement of the carrier sensing to optimize the power consumption, especially in cases where interferences to other communication are ex-

pected. The presented architecture has been achieved with off-the-shelf components.

# 3 Wake-Up Radio Circuit Components

## 3.1 Carrier Sensing Design Blocks

Figure 1 shows the block diagram of the circuit. The signal or electromagnetic waves are received via the antenna. They characterize due to low amplitude, high noise figure, and various interferences. Usually, a bandpass filter is used to pass only signals of the desired frequency bands. Nevertheless, in-band interferences between different systems in the same environment can be expected.

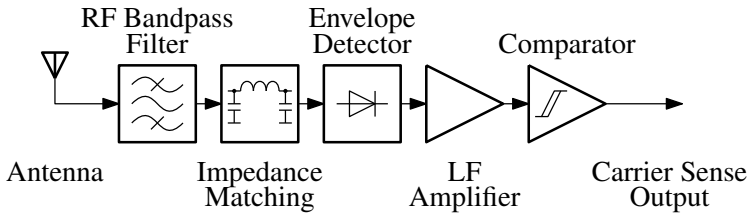


Figure 1: Block diagram of the analog part of the carrier sensing circuit. The main components are antenna, RF bandpass filter, impedance matching, envelope detector, LF amplifier, and comparator.

In the case of the proposed circuit, the 868 MHz band is used by choosing an appropriate surface acoustic wave (SAW) filter. The input and output impedance of this filter is typically 50 Ω. No additional matching is needed when using an antenna with this line impedance. To reduce the reflected power by the following diode envelope detector an impedance matching is needed. It is used to match the diodes' impedance to 50 Ω.

An envelope detector performs signal detection and conversion to a LF signal. Due to passive detection by using diodes the power consumption is as low as possible. The envelope detector is built by using two diodes in a Greinacher voltage doubler configuration. A following low-pass filter is added to remove the additional RF components of the rectified signal. The LF amplifier circuit is needed to boost the output voltage to a level, which is detectable by the following comparator. The current consumption of the used operational amplifiers (Op-Amps) is very important to meet the current consumption constrains [BDK18b]. A comparator is used to generate the digital carrier sense output signal from the amplified envelope signal. The output of the amplifier circuit is compared with a low reference voltage generated by a voltage divider.

## 3.2 Envelope Detector

The output of the envelop detector circuit is a voltage signal. It depends on the received input power. The output level of this circuit $V_d$ can be estimated by the equation 1 with $\gamma$ is the typical voltage sensitivity of the diode and $P_{in}$ the received RF power. The voltage doubler causes factor two.

$$V_D = 2 \cdot \gamma \cdot P_{in} \tag{1}$$

A typical figure of $\gamma$ is around $40\,mV/\mu W$. This results into a diode voltage of around $800\,\mu V$ at an input power of $-50\,dBm$.
The sensitivity of the diode is limited by a temperature-dependent noise of the component. The amplitude of the noise signal determines the accuracy of the lower sensitivity limit. The noise voltage $V_n$ of the diode can be expressed by the following equation:

$$V_n = \sqrt{4 \cdot k \cdot T \cdot B_V \cdot R_V} \tag{2}$$

where $T$ is the temperature, $k$ the Boltzmann constant, $R_V$ the video resistance and $B_V$ the bandwidth.
The tangential signal sensitivity (TSS) is used to describe the sensitivity of the detector diodes and is the lowest input signal power level $P_{TSS}$. At a signal level corresponding to the TSS value, the signal-to-noise ratio at the output is about 8 dB [MG86]. The voltage sensitivity $\gamma$ indicates the efficiency of the diode in converting the input power into a usable voltage [Agi03]. Thus, $P_{TSS}$ is calculated as follows:

$$P_{TSS} = \frac{2.5\sqrt{4 \cdot k \cdot T \cdot B_V \cdot R_V}}{\gamma} \tag{3}$$

Schottky diode detectors are commonly used as amplitude demodulators and level detectors in wireless and other RF and microwave signal processors [Sky08]. Detector designs are simple to realize using low-cost, plastic packaged, silicon Schottky diodes.

## 3.3 Low-Frequency Amplifier

### 3.3.1 Operational Amplifier Product Selection

The signal amplification is implemented by using general-purpose Op-Amps. The most important two properties of this Op-Amp are the gain bandwidth product

(GBWP) and the current consumption, which are highly dependent on each other. When choosing the right Op-Amps for the circuit a trade-off between current consumption and reaction time has to be made. A lower current consumption means a lower GBWP. A low GBWP results into a slow reaction time because of a slower settling time of the Op-Amps. To convert the GBWP to the settling time $t_{\text{settle}}$ the equation 4 can be used as an approximation.

$$t_{\text{settle}} \approx 3\tau = \frac{3}{\omega_{\text{k}}} = \frac{3}{2\pi \cdot f_{\text{k}}} = \frac{3 \cdot A_{\text{F}}}{2\pi \cdot \text{GBWP}} \tag{4}$$

Where $\tau$ represents the time constant, $\omega_{\text{k}}$ the angular low-pass filter cut-off frequency and $f_{\text{k}}$ the cut-off frequency and $A_{\text{F}}$ the voltage amplification factor.

### 3.3.2 Circuit Design

There are typically two ways to design an amplifier circuit with Op-Amps: using an inverting or a non-inverting design.
Using the inverting amplifier is not an obvious choice. Because several measures can be taken to re-invert the signal, the inverting amplifier is a possible choice too (e. g. inverting the diode signal, daisy-chaining multiple amplifiers). The first main difference between these amplifier circuits is the input impedance. The input impedance of the non-inverting amplifier is determined by the Op-Amp. The inverting amplifier's input impedance is approximately equal to the value of the resistor at the input. A lower input impedance increases the load on the RF part of the circuit.
The second main topic that needs to be considered when designing the amplifier circuit and choosing the Op-Amps, is the input and output voltage span of the circuit. To reduce the complexity of the needed power circuitry a single-rail supply is used. When using the non-inverting circuit so-called rail-to-rail inputs and outputs are mandatory, because of the low input signal level of the circuit. Without rail-to-rail inputs and outputs, small signals cannot be amplified by the Op-Amp. When using the inverting circuit a biasing of the amplification circuit is needed. Otherwise, positive input signals would result in negative output signals, which are not inside the Op-Amp's output range. This is done by adding a voltage source to the positive output of the Op-Amp [HH15].
The idea of using the non-inverting amplifier circuit in our proposed circuit design is to reduce the number of needed components. The disadvantage of this circuit is a problem with the Op-Amp's input voltage offset, we discovered with the help of experiments with the proposed circuit. Because commercially available Op-Amps in the very low current range ($< 1\,\mu\text{A}$) have a very high offset voltage relative to

the expected input voltages of around 800 µV, a so-called biasing circuit has to be added. This circuit is seen in figure 2 and consists of components $R_1$, $R_2$ and $C_1$.

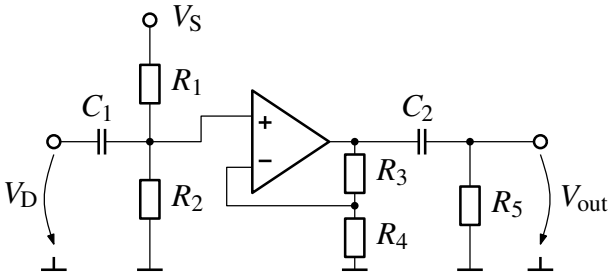


Figure 2: Schematic of the LF amplifier. Consisting of the biasing circuit on the left, the non-inverting amplifier circuit and the high-pass filter on the right.

The resistance of $R_1$ is in the order of 10 MΩ to ensure low current consumption of this biasing circuit. The resistance of $R_2$ is determined by the desired voltage drop and can be calculated by the corresponding voltage divider formula. The voltage drop has to be high enough to ensure proper compensation of the offset voltage of the Op-Amps. If the bias voltage is too high the maximum output voltage will be exceeded or an additional current will flow through the feedback resistors $R_3$ and $R_4$. After each amplification stage, a high-pass filter is added. This high-pass filter ensures that both the offset of the biasing circuit and the input offset of the Op-Amps are removed properly.

## 3.4 Comparator Circuit

When selecting the appropriate comparator for the circuit, the specifications of current consumption, propagation delay, and input offset voltage are the most important. When examining the commercially available comparators, it is noticeable that the propagation delay is highly dependent on the current consumption. Comparators with a low current consumption have a higher propagation delay. The typical input offset voltage of a sub-microampere comparator is in the range of several millivolts. To convert the output voltage of the amplifier circuit to a digital signal, a comparator with a static threshold voltage is used. The schematic can be seen in figure 3.

The threshold voltage is significantly higher than the input offset voltage of the comparator to ensure stable results between different comparators. To select the desired RF power threshold both this threshold voltage and the amplifier gain should be adjusted.

The digital output voltage of the comparator circuit $V_{CS}$ represents the carrier sensing output. This output signal can be read by a microcontroller.

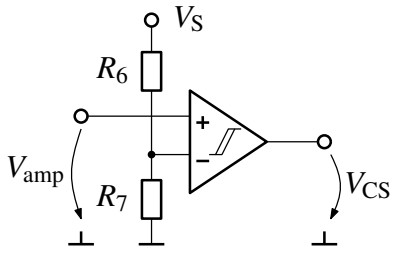


Figure 3: Schematic of the comparator circuit. The output signal of the LF amplifier is compared with a static threshold voltage. This voltage is generated by the voltage divider consisting of $R_6$ and $R_7$.

# 4 Circuit Design and Experimental Setup

This section presents a possible implementation of the carrier sense circuit. Multiple tests are presented and a way of setting the right parameters for such a design.

## 4.1 Diode Comparison

The diode HSMS-2852 from Agilent Technologies is the typical diode used in the envelope detector by multiple other publications [BD14] [Mag+16] [ABD15]. Because this diode is discontinued by the manufacturer a replacement diode is needed. The SMS7630-006LF from Skyworks Solution Inc. has nearly identical parameters and the following investigations were made, to ensure that the diode SMS7630 is a good replacement diode. First of all, the noise voltage, noise level and TSS were calculated accordingly by equations 2 and 3 and can be seen in table 1. These values differ only slightly.

Table 1: Noise and TSS of detector diodes

| | HSMS-2852 | SMS7630 |
|---|---|---|
| $V_n$ [µV] | 1.57 | 1.27 |
| Noise level [dBm] | –83 | –85 |
| $P_{TSS}$ [dBm] | –70 | –72 |

With the help of the following experiment the voltage sensitivity curve was measured. For both diodes a printed circuit board (PCB) was made. Figure 4 shows one of these boards. The used circuit consists of a matching circuit, the diode, and a low-pass filter with resistive load at the end.
In figure 5 the block diagram of the measurement setup is seen. The signal generator produces a RF carrier pulse of a length of 5 ms. The power of the signal generator can be adjusted and is measured by a spectrum analyzer. The test signal is fed into one of the test boards. An oscilloscope measures the output signal.

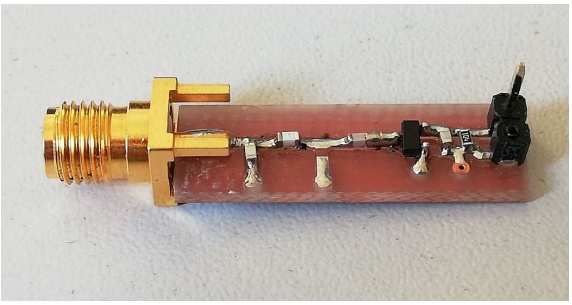

Figure 4: Picture of the PCB used for the diode selection tests. From left to right: SMA connector, matching circuit, diode, low-pass filter with resistive load.

A typical output response can be seen in figure 6. This picture was captured at a RF power of −30 dBm with the diode HSMS-2852.

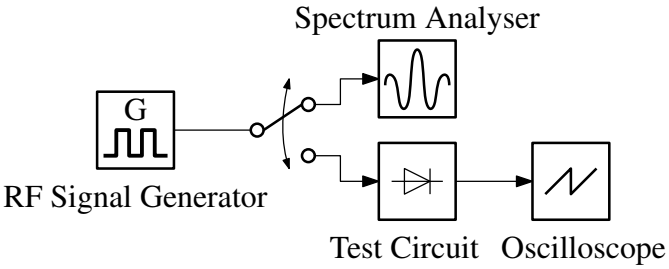


Figure 5: Block diagram of measurements for the diode comparison

To compare both diodes the amplitude of the resulting envelope waveform was captured at multiple voltage levels. The results are seen in figure 7. It is worth mentioning that the signal at an output power of −37.8 dBm is the last measurable by our setup. For measuring at lower input levels, an additional preamplifier is needed. The experiment showed that the transmission properties of both diodes are nearly identical. Especially at lower input powers, the voltage sensitivity curves match exactly. A typical voltage sensitivity of both diodes is $\gamma = 80\,\mathrm{mV}/\mu\mathrm{W}$. This test shows that the diode SMS7630-006LF is a good replacement for the HSMS-2852. For the following tests, in the envelope detector circuit, the SMS7630 is used.

## 4.2 Radio Frequency Circuit

The schematic of the RF circuit can be seen in figure 8. An SMA connector realizes the RF input. It allows the connection to both a signal generator or an antenna. The SAW filter is a typical filter for the 868 MHz band. The components $L_1$ and $C_1$ match the impedance of the envelope detector to 50 Ω. As described previously, a Greinacher voltage doubler boosts the performance of the envelope detector. The output voltage is converted and filtered by the components $R_1$ and $C_3$. These components act as a low-pass filter. Only the LF components of the signal are

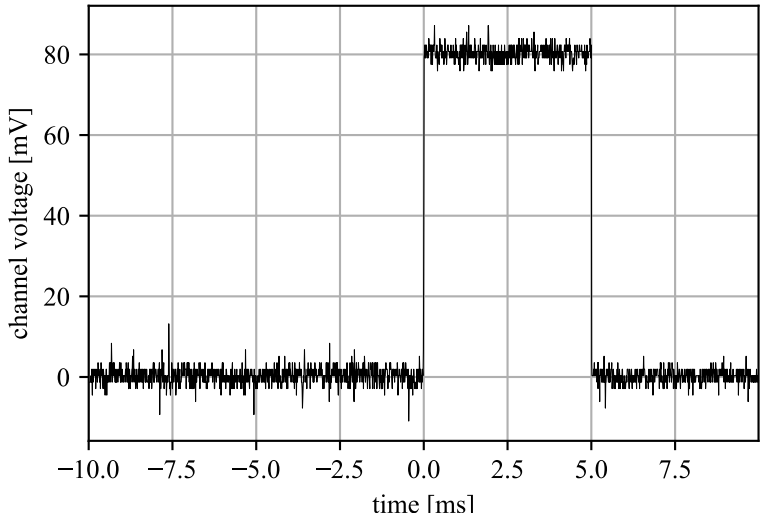


Figure 6: Typical waveform of the envelope detector output generated by a 5 ms carrier pulse. Captured by an oscilloscope, a test circuit with the HSMS2852 diode at a RF power of −30 dBm.

remaining.

In comparison to the previous test circuits, a SAW filter is added. To show the impact of the SAW filter on the voltage sensitivity of the circuit, the previously made tests were repeated with this circuit. The test results can be seen in figure 9. The output voltage with the SAW filter is significantly smaller. The additional transmission losses introduced by the filter explain this behavior. This trade-off has to be made to ensure proper filtering of the RF signal against signals on other frequency bands.

The average voltage sensitivity of the proposed RF part can be calculated from the experimental results and is about 28 mV/µW. It can be estimated that an output voltage of around 280 µV is generated at a RF input power of –50 dBm. This figure will be used to define the parameters of the amplifier and comparator circuit.

## 4.3 Test Circuit

In figure 10 a picture of the test PCB can be see. The RF circuit in the upper part was specially matched for the PCB. In the lower part, the LF circuit is implemented. The two Op-Amps and the comparator are populated.

The table 2 shows the parameters of the used comparator. The threshold voltage was set to 100 mV because of the maximum input offset voltage of the comparator. The table 3 shows the parameters of the amplification circuit. A total amplification of factor 900 achieves a carrier sensing at input powers less than –50 dBm. Two stages in series realize this amplification. The resulting settling time was

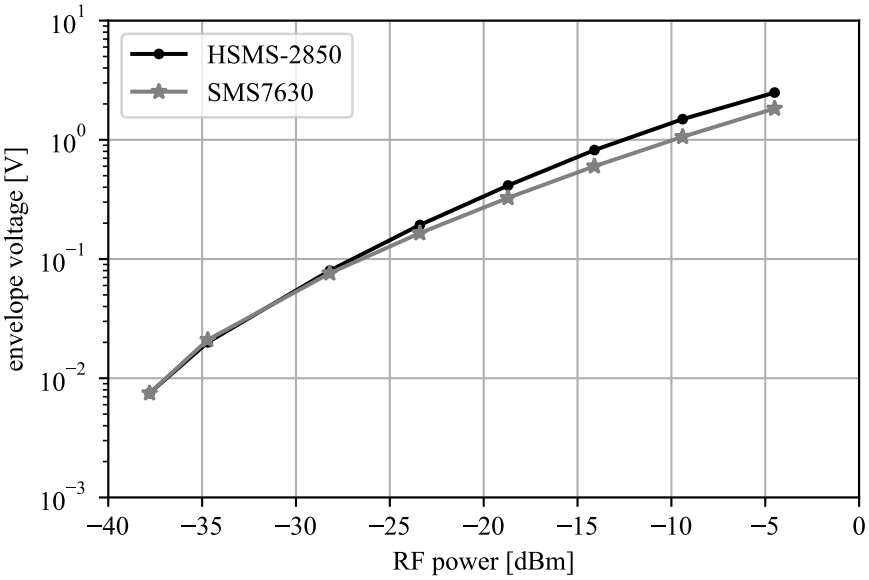


Figure 7: Voltage sensitivity curve of the two selected diodes

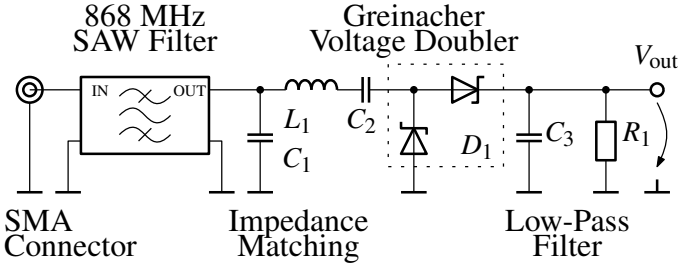


Figure 8: Schematic of the RF part of the proposed implementation of the carrier sensing circuit

calculated with equation 4. The biasing voltage was selected according to the Op-Amp's input offset voltage.

To ensure that the circuit is working properly the typical test procedure described early was repeated. Both output signals of the amplification stages were monitored. The results of this test can be seen in figure 11.

The amplification of the test signal was measured to a minimum input power of –47 dBm. The amplitude of the signal reached 165 mV. This output signal together with the comparator output can be seen in figure 12.

Table 2: Parameters of the comparator circuit

| | |
|---|---|
| Supply voltage | 3.0 V |
| Comparator | TLV3691 |
| Typical current consumption | 75 nA |
| Typical propagation delay | 45 µs |
| Maximum input offset voltage | ±15 mV |
| Threshold voltage | 100 mV |

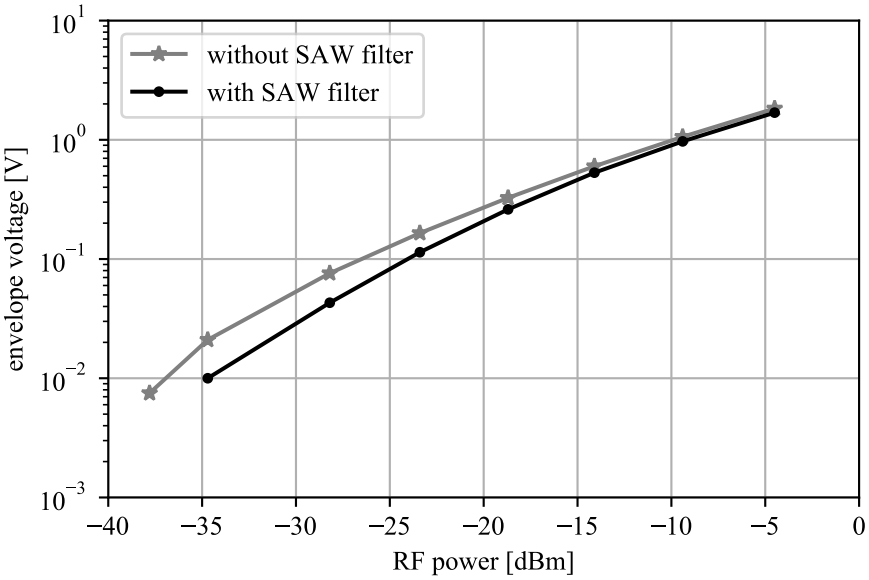


Figure 9: Voltage sensitivity curve with and without the SAW filter

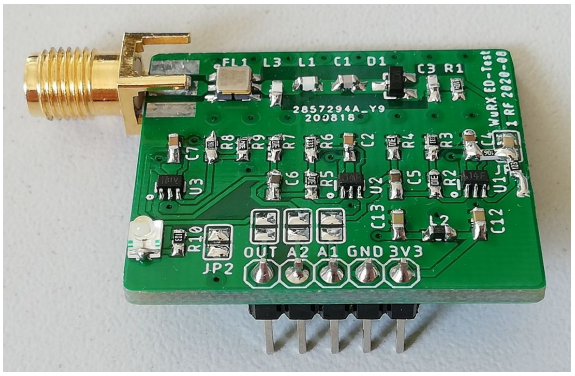


Figure 10: Picture of the PCB used for the system test

For greater input signals the output signal is clamped to the supply voltage, but the comparator output is still present. The calculation of the power consumption can be seen in table 4. This total power consumption of around 1.4 µA was also verified by a bench multimeter.

## 4.4 Usage as a Wake-Up Receiver

The proposed carrier sensing circuit can be used on both sides of the transmission chain. The first usage - on the transmitter side - is carrier detection. The second usage - on the receiver side - is an ultra-low-power wake-up receiver.
To test the usability of the circuit as a wake-up receiver a radio transceiver module is used. A carrier pulse at the center frequency of 868.0 MHz at an output power of 10 dBm is generated. Two λ/2 whip antennas are used for the transmitter and the carrier sensing test circuit. On the output of the test circuit, a LED is added. With this setup, a maximum transmission range of around 10 m can be observed.

Table 3: Parameters of the amplifier circuit

| | |
|---|---|
| Total amplification factor | 900 |
| Number of amplifier stages | 2 |
| Amplification per stage | 30 |
| Operational amplifier | TLV521 |
| Typical current consumption | 350 nA |
| Typical GBWP | 6 kHz |
| Maximum input offset voltage | ±3 mV |
| Settling time | 2.4 ms |
| Biasing voltage | 3 mV |

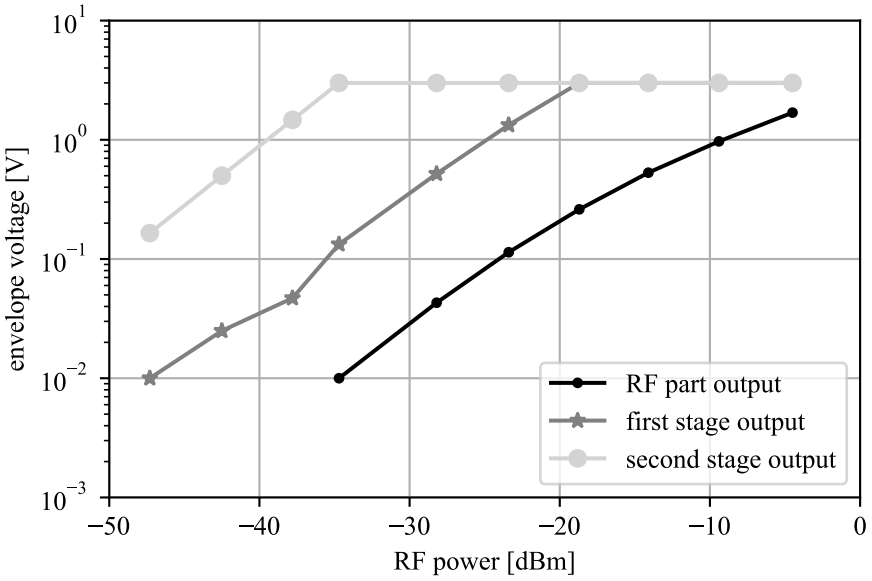


Figure 11: Voltage sensitivity curve of RF circuit and both amplifier stages

Interferences of other RF systems are present but less frequent.

# 5 Discussion and Conclusion

## 5.1 Further work

The proposed carrier sensing circuit shows a simple way to implement a wake-up receiver without any specialized integrated circuits, like microcontrollers or LF wake-up receiver chips. The RF part of the circuit is kept simple. Additional work in the LF amplification circuit has to be done. More tests have to be made, to investigate whether the power consumption can be reduced by using the inverting amplifier. Theoretically, the biasing circuit can be replaced by an ultra-low power voltage regulator. Additional power savings for the comparator threshold generation are possible too.

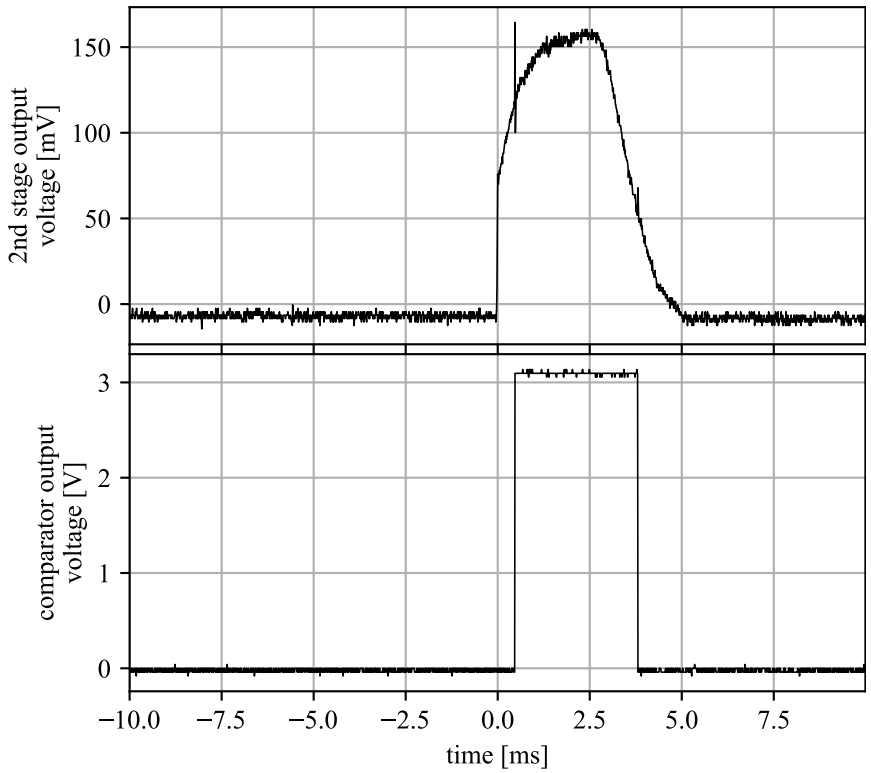


Figure 12: Typical waveform of the second amplifier stage output and the comparator signal. Captured by an oscilloscope, the carrier sensing test circuit at a RF power of –47 dBm.

Table 4: Calculated current consumption of the proposed carried sensing circuit

| Component | I [nA] |
|---|---|
| Biasing Circuit | 300 |
| Amplifier | 700 |
| Comparator | 75 |
| Comparator threshold generation | 300 |
| Total | 1375 |

Currently, the circuit was only built for a carrier frequency of 868 MHz. By swapping the SAW filter and matching the RF circuit other frequency bands can be used. Further tests will be made to test the circuit's performance in the 433 MHz and 2.4 GHz range. The 2.4 GHz range is highly important due to its capability to realize high data rate transmissions.

The transmission loss of the RF signal and the resulting range is dependent on the wavelength. This can be explained by the Friis transmission formula, seen in equation 5 where $P_r$ and $P_t$ are the received and transmitted power, $A_r$ and $A_t$ the effective aperture of the corresponding antennas, $d$ the distance, and $\lambda$ the

wavelength.

$$\frac{P_\mathrm{r}}{P_\mathrm{t}} = \frac{A_\mathrm{r} \cdot A_\mathrm{t}}{d^2 \cdot \lambda^2} \tag{5}$$

The effect of the lower transmission range has to be observed and what applications are suitable when using the circuit at 2.4 GHz.

## 5.2 Usability as a Wake-Up Receiver

As described in section 4.4 a carrier pulse of 5 ms can be used as a wake-up signal and can be received within a range of 10 m. Because no additional filter techniques are applied (e. g. modulation frequency detection or address matching) all RF packages with matching power and duration are detected.
This is why this circuit is specialized for an environment with low interferences from other RF components. When there are only a few participants in the wireless network address filtering is not needed. The latency and current consumption of these wireless networks can be reduced significantly. We are planning to use this circuit for a measurement system located inside a shielded machine gearbox. In this use case interferences are very low. The benefits of the implementation lie in a significant decrease in power consumption and latency time. When using this circuit in a different environment, it is clear, that further filtering techniques are needed.

## 5.3 Usability as a Carrier Sense Circuit

The second usage is found in carrier detection and collision avoidance techniques. When communicating in a wireless network package collision is quite frequent. These collisions result in an energy loss because the current package needs to be resent.
This energy loss $E_\mathrm{loss}$ through one package collision can be approximated by the equation 6. The collision probability $p_\mathrm{col}$ was estimated at 30 %, the package duration $t_\mathrm{P}$ at 5 ms, the transmission current consumption $I_\mathrm{T}$ at 25 mA and the supply voltage $V_\mathrm{S}$ at 3.3 V.

$$E_\mathrm{loss} = p_\mathrm{col} \cdot t_\mathrm{P} \cdot I_\mathrm{T} \cdot V_\mathrm{S} = 124\,\mu\mathrm{J} \tag{6}$$

To put this value of 124 µJ into relation, the time, which the carrier sense circuit

can stay active with this energy, can be calculated by equation 7.

$$t_{\text{active}} = \frac{E_{\text{loss}}}{V_S \cdot I_S} = 26.8\,\text{s} \tag{7}$$

Because the carrier sense circuit is only used a fraction of a time to ensure no carrier is active on the channel, the carrier sense circuit's power loss is nearly negligible. Modern wireless transceiver modules often have a carrier sensing circuit, clear channel assessment module, or wake-on radio integrated. The improvement is much better sensitivity and selectivity. But when taking a look at typical current consumptions of these modes, they are in the order of 10 mA [Atm14]. Comparing this current consumption to the current consumption of the proposed circuit it is very clear that an improvement of factor 7000 can be achieved.

## 5.4 Conclusion

In this work, a power-saving approach with energy detection and carrier sensing is presented. When using the circuit in a receiver it turns on only when a carrier signal is detected at a carrier frequency of 868 MHz. This setup observes a maximum transmission range of around 10 m and total power consumption of 4.2 µW. Further development of the circuit is planned not only to be used at 868 MHz but also to be designed for other frequency bands. Further tests will be made to test the circuit's performance in the 433 MHz and 2.4 GHz range. The 2.4 GHz range is very important due to its capability to realize high data rate transmissions.

# References


[Agi03] Agilent Technologies. *Agilent RF and Microwave Test Accessories: Detector Overview*. Ed. by Agilent Technologies. 2003.

[ABD15] Yasmin Ammar, Sadok Bdiri, and Faouzi Derbel. "An ultra-low power wake up receiver with flip flops based address decoder". In: *2015 IEEE 12th International Multi-Conference on Systems, Signals & Devices (SSD15)*. IEEE, 2015, pp. 1–5. DOI: 10.1109/SSD.2015.7348127.

[Atm14] Atmel. *AT86RF233 - Low Power, 2.4GHz Transceiver for ZigBee, RF4CE, IEEE 802.15.4, 6LoWPAN, and ISM Applications*. 2014. URL: http://ww1.microchip.com/downloads/en/DeviceDoc/Atmel-8351-MCU_Wireless-AT86RF233_Datasheet.pdf.

[Ban16] Amir Bannoura. *Algorithms and applications for low power wireless sensor networks using wake-up receivers*. Jan. 2016.

[BBD18] Sadok Bdiri, Oussama Brini, and Faouzi Derbel. “Digital Back-end Based on a Low-power Listening Protocol for Wake-Up Receivers”. In: *Sensors & Transducers*. Vol. 224. 2018, pp. 22–27. URL: http://www.sensorsportal.com/HTML/DIGEST/P_3001.htm.

[BD14] Sadok Bdiri and Faouzi Derbel. “A nanowatt Wake-Up Receiver for industrial production line”. In: *2014 IEEE 11th International Multi-Conference on Systems, Signals & Devices (SSD14)*. IEEE, 2014, pp. 1–6. DOI: 10.1109/SSD.2014.6808911.

[BDK18a] Sadok Bdiri, Faouzi Derbel, and Olfa Kanoun. “A Tuned-RF Duty-Cycled Wake-Up Receiver with –90 dBm Sensitivity”. In: vol. 18. 2018. DOI: 10.3390/s18010086.

[BDK18b] Sadok Bdiri, Faouzi Derbel, and Olfa Kanoun. “A wake-up receiver for online energy harvesting enabled wireless sensor networks”. In: *Energy Harvesting for Wireless Sensor Networks*. Ed. by Olfa Kanoun. De Gruyter, 2018, pp. 305–320. ISBN: 9783110436112. URL: https://www.degruyter.com/viewbooktoc/product/462297.

[DP+16] Diego Del Prete Massimo an Masotti et al. “A dual-band wake-up radio for ultra-low power Wireless Sensor Networks”. In: *2016 IEEE Topical Conference on Wireless Sensors and Sensor Networks*. Piscataway, NJ: IEEE, 2016, pp. 81–84. ISBN: 978-1-5090-1691-4. DOI: 10.1109/WISNET.2016.7444328.

[HH15] Paul Horowitz and Winfield Hill. *The Art of Electronics*. 3rd. USA: Cambridge University Press, 2015. ISBN: 0521809266.

[Mag+16] Michele Magno et al. “Design, Implementation, and Performance Evaluation of a Flexible Low-Latency Nanowatt Wake-Up Radio Receiver”. In: *IEEE Transactions on Industrial Informatics* 12.2 (2016), pp. 633–644. ISSN: 1551-3203. DOI: 10.1109/TII.2016.2524982.

[MG86] H. Meinke and Friedrich-Wilhelm Gundlach. *Taschenbuch der Hochfrequenztechnik*. Vierte, völlig neubearbeitete Auflage. Berlin, Heidelberg: Springer Berlin Heidelberg, 1986. ISBN: 9783642968945. DOI: 10.1007/978-3-642-96894-5. URL: https://books.google.de/books?id=3BrUBgAAQBAJ.

[Ple08] Nathan Pletcher. *Ultra-low power wake-up receivers for wireless sensor networks: Dissertation*. University of California at Berkeley, 2008.

[Pol+16] Tommaso Polonelli et al. “A wake-up receiver with ad-hoc antenna co-design for wearable applications”. In: *SAS Sensors Applications Symposium*. Piscataway, NJ: IEEE, 2016, pp. 1–6. ISBN: 978-1-4799-7250-0. DOI: 10.1109/SAS.2016.7479632.

[Sky08] Skyworks Solutions, Inc. *Mixer and Detector Diodes*. Ed. by Skyworks Solutions, Inc. 2008. URL: https://www.skyworksinc.com/-/media/SkyWorks/Documents/Products/1-100/200826A.pdf.

[Spe+15] Dora Spenza et al. “Beyond Duty Cycling: Wake-up Radio with Selective Awakenings for Long-lived Wireless Sensing Systems”. In: Apr. 2015. DOI: 10.1109/INFOCOM.2015.7218419.